Matching of Observational Accuracy and Sampling Resolution in Meteorological Data Acquisition Experiments[1]

M. A. ALAKA AND R. C. ELVANDER

Techniques Development Laboratory, NOAA/National Weather Service, Silver Spring, Md. 20910

(Manuscript received 21 September 1971, in revised form 20 January 1972)

ABSTRACT

On the basis of a 10-year record of rawin observations in the Caribbean, experiments were carried out to determine the appropriate matching between the accuracy and density of meteorological observations.

The results indicate that at 850 mb, if the distance between neighboring stations is of the order of 800 km or more, it makes little difference whether the random errors of observations are 2 kt or twice this amount. This is especially true if the observations are used to construct a regular grid of interpolated values. At 200 mb, an even larger range of observational errors is permissible if the distance between stations is large. The experiments further demonstrate that the distance between the raw observations must be smaller than that between the reconstructed grid points if the field gradients are to be computed with reasonable accuracy.

As the scale of interest becomes smaller, accuracy requirements become more stringent. For instance, if we can measure the zonal wind components at 850 mb in January with an accuracy of 3 kt and if we have two observations 100 km apart, there is only a 0.2 probability that the error in the measured difference between the two observations is equal to or less than one-fifth of the true difference. To increase this probability to 0.4, the accuracy of the measurement must be within 1 kt. Similarly, if the rms error of temperature observations, 100 km apart, is 1C, the probability is 0.15 that the error in the measured difference is equal to or less than one-fifth of the true. On the other hand, if the rms observation error is only 0.1C, the probability is 0.6 that the error is equal to or less than one-fifth of the true difference.

The study is intended to provide planners of meteorological data acquisition experiments with some insight into the options at their disposal. Thus, for field experiments designed to delineate broad-scale atmospheric features, it should help identify the point of diminishing returns for instrumental accuracy. Conversely, if only a given instrumental accuracy is obtainable, it should provide an estimate of the maximum useful sampling resolution.

1. Introduction

One of the main components of the Global Atmospheric Research Program (GARP) is a series of data acquisition experiments designed to promote a better understanding of the structure, behavior and interaction of atmospheric phenomena of different scales. Among the many problems facing planners of these experiments is the correct matching of observational accuracy with the density and frequency of observations in the different experiments.

In general, experiments designed to delineate the large-scale atmospheric features do not require a high order of observational accuracy. If the scale of interest is sufficiently large, it is pertinent for planners to ask how far it is useful to push the accuracy of observations for a given sampling resolution (COSPAR Working Group 6, 1971).

As the scale of interest becomes smaller and smaller and the sampling resolution is increased, accuracy requirements become more and more stringent. The reason is that measurements close together in space or time must bring out small differences in the numerical values of the sampled element, and unless the measurements are sufficiently accurate, these small differences could be submerged in the observational "noise." Thus, for high-resolution experiments, the pertinent question is how far is it useful to push the sampling resolution with a given level of observational accuracy.

On the basis of a 10-year record of rawin observations from some 35 stations in the Caribbean, we have carried out some numerical experiments which provide an insight into the above problems. Although, strictly speaking, the results and conclusions apply only to the small area from which the observations were taken, they are probably valid for other tropical areas. Furthermore, the same methodology may be applied to the design of data acquisition systems for field experiments in other regions where reasonably long climatological records are available.

2. Reconstructing atmospheric fields

The efficacy of an array of meteorological observations may be assessed from the accuracy with which the

[1] Presented at the Seventh Technical Conference on Hurricanes and Tropical Meteorology, 6–9 December 1971, St. Michael, Barbados, West Indies.

atmospheric fields sampled by these observations may be reconstructed. In general, the reconstruction process consists of generating a regular lattice of representative values of these fields, which may be used as input to numerical forecasting models or to perform other computations.

A convenient manner of evaluating this capability is provided by application of the theory of optimum interpolation (Gandin, 1963) which requires a knowledge of the statistical structure of the fields which are being reconstructed and of the random errors inherent in the observations used in the reconstruction.

a. Theory of optimum interpolation

Let $\mathbf{r}_i=\mathbf{r}_0, \mathbf{r}_1, \cdots, \mathbf{r}_n$ denote a set of independent vectors defining the location of points in a sampling space. Consider a function $f(\mathbf{r})$ whose sampled values $\hat{f}_i=\hat{f}_1, \hat{f}_2, \cdots, f_n$ have a error $\epsilon_i=\epsilon_1, \epsilon_2, \cdots, \epsilon_n$ so that

$$\hat{f}_i=f_i+\epsilon_i. \tag{1}$$

We wish to determine the value f_0 at some location $\mathbf{r}_0$ from the measured values $\hat{f}_i$. If f_0' and fi' denote the deviation of f_0 and f_i from their respective mean, we may express f_0' in terms of the linear combination

$$f_0'=\sum_{i=1}^{n}(f_i'+\epsilon_i)P_i+I_0, \tag{2}$$

in which P_i are the weighting factors and I_0 the error in determining f_0' by interpolation from $\hat{f}_i$.

The mean square interpolation error is

$$\mathcal{E}=\overline{I_0^2}=\overline{[\sum_{i=1}^{n}(f_i'+\epsilon_i)P_i-f_0']^2}. \tag{3}$$

We make the usually satisfactory assumption that the random errors ϵ_i are:

1) Unrelated to the true values of the measured quantities, i.e.,

$$\overline{\epsilon_i f_i'}=0. \tag{4}$$

2) Unrelated to each other, i.e.,

$$\overline{\epsilon_i\epsilon_j}=\begin{cases}0, & \text{when } i\neq j\\ \sigma_{\epsilon_i}^2, & \text{when } i=j\end{cases} \tag{5}$$

where $\sigma_{\epsilon_i}^2$ denotes the mean-square random observation errors.

The above assumptions imply that the random errors do not affect the values of the true covariances but inflate the true variances σ_i^2 by an amount $\sigma_{\epsilon_i}^2$.

By invoking assumptions (4) and (5), we can rewrite Eq. (2) as

$$\mathcal{E}=\sum_{i=1}^{n}\sum_{j=1}^{n}\overline{\hat{f}_i'\hat{f}_j'}P_iP_j+\sum_{i=1}^{n}\sigma_{\epsilon_i}^2P_i^2-2\sum_{i=1}^{n}\overline{\hat{f}_i'f_0'}P_i+\sigma_0^2. \tag{6}$$

The optimum weights p_i corresponding to a minimum value of $\mathcal{E}$ are obtained by setting

$$\frac{\partial\mathcal{E}}{\partial P_i}=0. \tag{7}$$

The weights thus form a system of linear equations

$$\sum_{j=1}^{n}\overline{\hat{f}_i'\hat{f}_j'}p_j+\sigma_{\epsilon_i}^2p_i=\overline{\hat{f}_i'f_0'},\quad i=1, 2, \ldots, n. \tag{8}$$

Denoting $\mathcal{E}_{\min}$ by E, and combining Eqs. (6) and (8), we have

$$E=\sigma_0^2-\sum_{i=1}^{n}\overline{\hat{f}_i'f_0'}p_i. \tag{9}$$

By virtue of assumption (5), $\overline{\hat{f}_i'\hat{f}_j'}$ and $\overline{\hat{f}_i'f_0'}$ are, respectively, equivalent to $\overline{f_i'f_j'}$ and $f_i'f_0'$; moreover, $\sigma_0^2=\hat{\sigma}_0^2-\sigma_{\epsilon_0}^2$ where $\hat{\sigma}_0$ is the computed variance.

We now make the convenient assumption that the variances are homogeneous and the covariances both homogeneous and isotropic. Eqs. (8) and (9) may then be written

$$\sum_{j=1}^{n}\mu_{ij}p_j+\lambda_i^2p_i=\mu_{0i},\quad i=1, \cdots n, \tag{10}$$

and

$$E=\sigma^2(1-\sum_{i=1}^{n}\mu_{0i}p_i), \tag{11}$$

where

$$\mu_{ij}=\frac{\overline{f_i'f_j'}}{\sigma^2}=\frac{\overline{\hat{f}_i'\hat{f}_j'}}{\hat{\sigma}^2-\sigma_\epsilon^2},$$

the autocorrelation coefficient between values of the function at locations $\mathbf{r}_i$ and $\mathbf{r}_j$,

$$\mu_{0i}=\frac{\overline{f_0'f_i'}}{\sigma^2}=\frac{\overline{f_0'\hat{f}_i'}}{\hat{\sigma}^2-\sigma_\epsilon^2},$$

the autocorrelation coefficient between values of the function at $\mathbf{r}_0$ and $\mathbf{r}_i$, and

$$\lambda_i^2=\frac{\sigma_{\epsilon_i}^2}{\sigma^2}=\frac{\sigma_{\epsilon_i}^2}{\hat{\sigma}^2-\sigma_{\epsilon_i}^2}.$$

From (10) and (11), we note that both the weights and the rms interpolation errors depend on the scale of the function as represented by the autocorrelations μ_{0i} and μ_{ij}, on the variability as represented by σ^2, and on the random error σ_{ϵ_i}. Eq. (11) shows that the mean-square interpolation error cannot exceed the variance of the function which is being interpolated.

b. Errors of optimum interpolation

We have used Eqs. (10) and (11) in a series of experiments to determine the error involved in estimating the value of the zonal wind component at a given location ⊗ by optimum interpolation from the nearest 12 observations located on a regular grid as shown in Fig. 1. Both the basic grid length X and the rms errors of observations were made to vary from experiment to experiment.

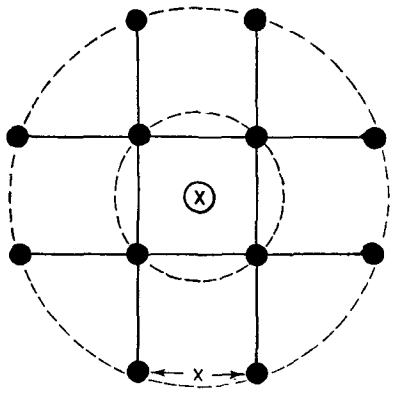

FIG. 1. The 12-point interpolation grid used in this study.

Effective optimization of the interpolation procedure depends on an accurate estimate of the variances and autocorrelations. Values of these parameters used in the present study are listed in Table 1. The manner in which these values were obtained is described in detail elsewhere (Alaka and Elvander, 1972).

As noted above, we have assumed that the variances are homogeneous and the covariances both homogeneous and isotropic. Fig. 2 indicates that neither assumption is strictly valid. Therefore, due allowance must be made for these assumptions in interpreting our results.

Figs. 3 and 4 show isopleths of the normalized error of interpolation, $Q=E^{\frac{1}{2}}/\sigma$, as a function of station separation for the zonal wind component U at 850 and 200 mb in January and July. In these figures, the curved

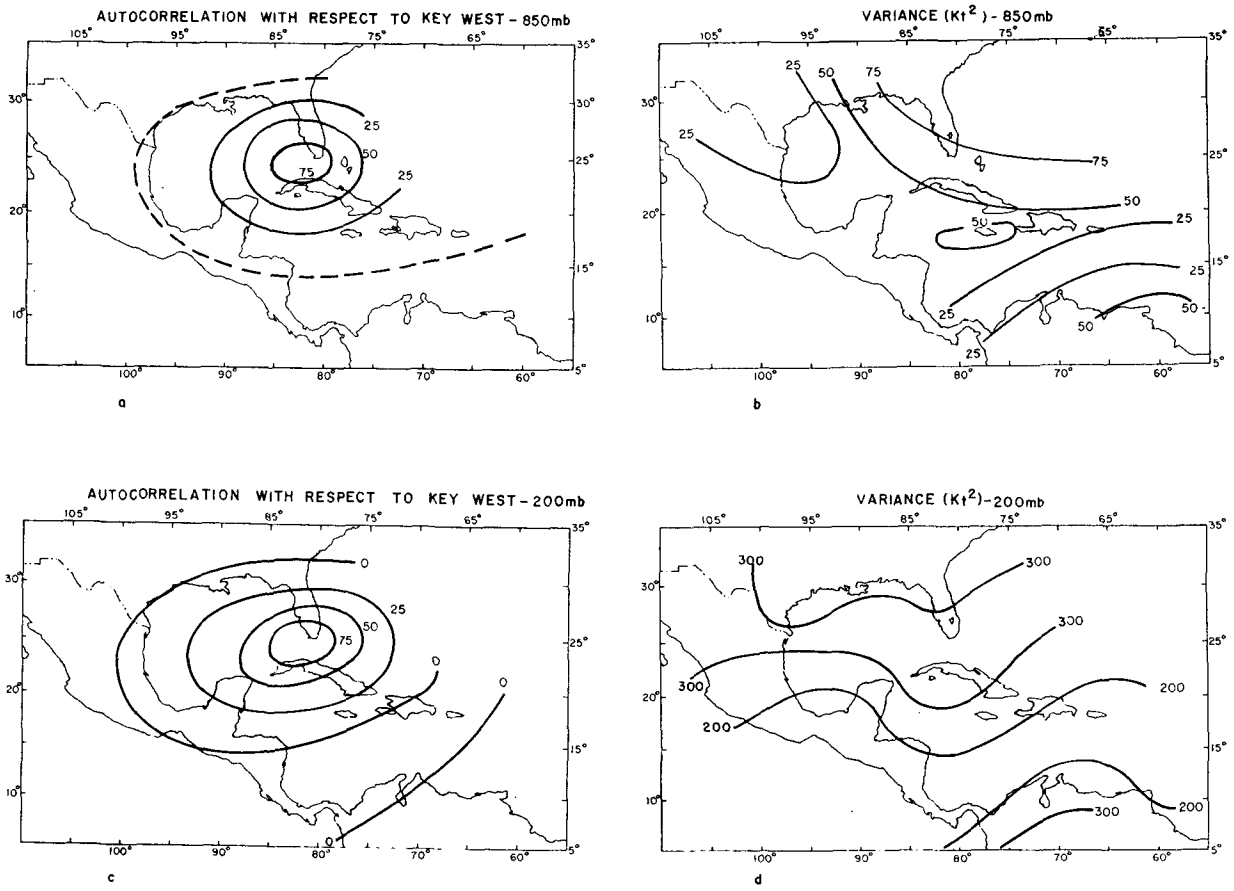

FIG. 2. Autocorrelations and variances of the zonal wind in July at 850 mb, a and b, and 200 mb, c and d.

TABLE 1. Isotropic autocorrelations and mean variances for the zonal wind component (U) and temperature in the Caribbean. The distance between pairs of stations is denoted by ρ.

Element	Month	Level (mb)	Autocorrelation	Variance
Zonal wind component (U)	January	850	$\mu=[1.44\exp(-0.537\,X^{0.802})-0.44]\cos 0.260\rho$	84.9 kt^2
		200	$\mu=[2.52\exp(-0.270\,X^{0.845})-1.52]\cos 0.292\rho$	579.0 kt^2
	July	850	$\mu=[0.895\exp(-2.12\,X^{1.06})+0.105]\cos 0.441\rho$	34.3 kt^2
		200	$\mu=[1.01\exp(-1.37\,X^{1.36})-0.01]\cos 0.985\rho$	241.0 kt^2
Temperature	January	850	$\mu=[1.67\exp(-0.346\,X^{1.43})-0.67\cos 0.354\rho$	10.3 (°C)^2
		200	$\mu=[0.94\exp(-0.780\,X^{1.17})+0.06\cos 0.127\rho$	7.1 (°C)^2
	July	850	$\mu=[0.869\,\mathrm{esp}(-2.82\,X^{1.06})+0.131]\cos 0.235\rho$	2.82 (°C)^2
		200	$\mu=[0.685\exp(-2.19\,X^{0.989})+0.315]\cos 0.215\rho$	3.99 (°C)^2

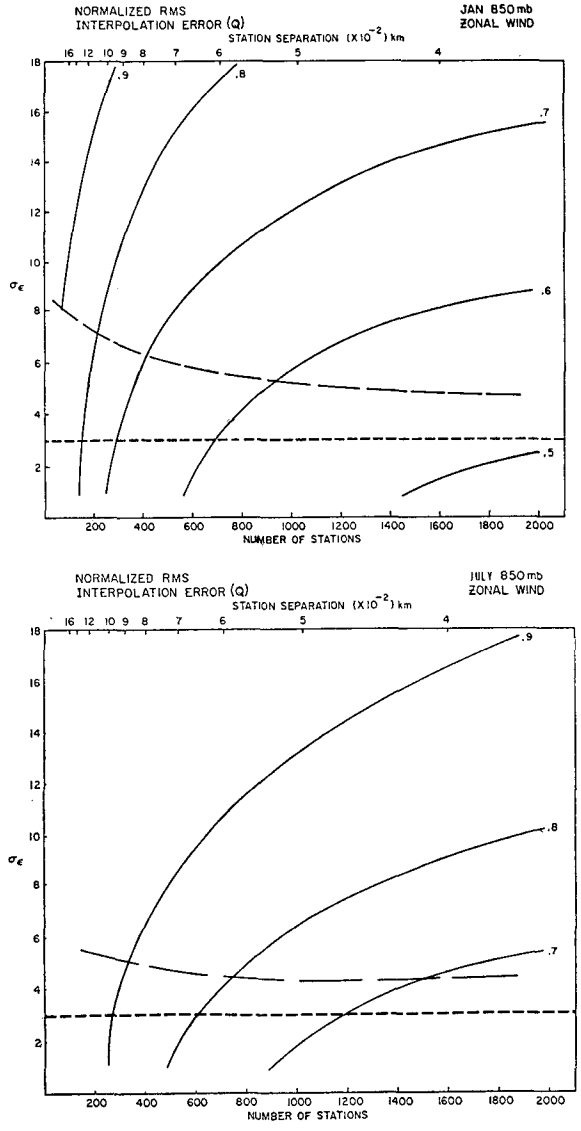

FIG. 3. Normalized interpolation errors ($Q=E^{\frac{1}{2}}/\sigma$) of the zonal wind at 850 mb as a function of the random errors of observation and of the number of stations in the tropical belt from 30N to 30S for a) January, a, and July, b. The dashed straight lines indicate the estimated present level of the rms random errors of rawin observations; the dahsed curves are the locus of points where $Q=\sigma\epsilon/\sigma$.

dashed line is the locus of points where $E^{\frac{1}{2}}=\sigma_\epsilon$. Below this line, the errors of interpolation exceed the random errors of observation; above the line, the interpolated

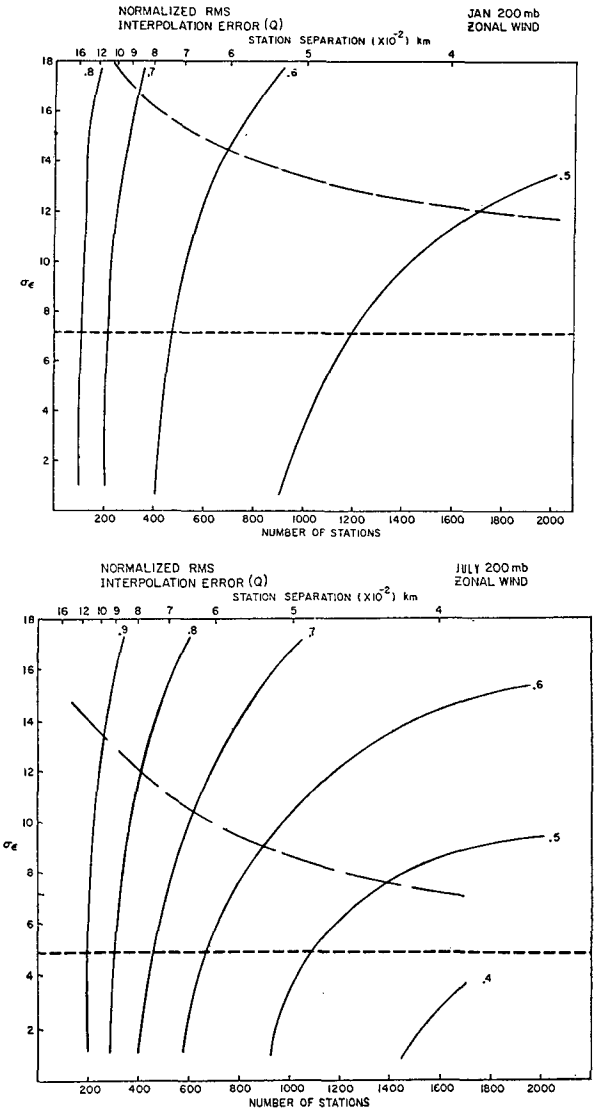

FIG. 4. Same as Fig. 3 except for 200 mb.

values are more accurate than the observations used in the interpolation. The less accurate the observations and the closer together they are, the more gain in accuracy is achieved by the interpolated values over the raw observations. The horizontal dotted lines in the figures indicate the estimated present level of the random errors of rawin measurements.

A common feature of Figs. 3 and 4 is that near the present level of the random errors of rawin observations (indicated by the dashed horizontal line), the isopleths of Q are almost vertical when the station separation is large. This indicates that decreasing the separation between observations is much more effective in reducing the errors of interpolation than is increasing the accuracy of observation. Indeed, at 850 mb, if the distance between neighboring observations is about 800 km or more, it makes very little difference for the accuracy of the interpolated values whether the random errors of observations are 2 kt or twice that amount. At 200 mb, the range of observational errors which are associated with comparable interpolation errors is even larger when the station separation is large. Under these circumstances there would seem to be very little point in attempting to provide very accurate observations especially if these involve added effort and expense.[2]

As the station separation decreases, the isopleth of Q tend to curve until they become quasi-horizontal when the grid distance is reduced, say to 400 km or less. Beyond this point, very little improvement is achieved by further reducing station separation. By the same token, any increase in the accuracy of interpolation can be achieved almost exclusively by increasing the accuracy of the raw observations.

c. *Network considerations*

Fig. 5 shows the variation of the rms interpolation errors of the zonal wind component as a function of the number of regularly spaced stations over the tropical zone between 30N and 30S. The scale at the top of the figure indicates the corresponding station separation in hundreds of kilometers. The estimated random errors of current rawinsonde observations listed in Table 2 have been used in the computations. The manner in which these errors were estimated is described elsewhere by the authors (Alaka and Elvander, 1972).

TABLE 2. Estimated rms random observation errors.

Element	Month	Level (mb)	rms error
Zonal wind component (U)	January	850	3.0 kt
		200	7.1 kt
	July	850	3.0 kt
		200	4.8 kt
Temperature	January	850	0.84C
		200	0.84C
	July	850	0.84C
		200	0.84C

[2] According to a recent study by Steinitz *et al.* (1970), this conclusion may not be valid for temperature and geopotential fields in the tropics.

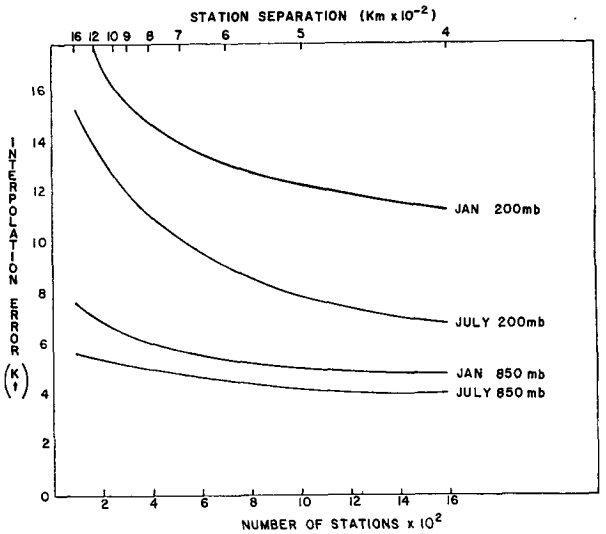

FIG. 5. Rms errors of optimum interpolation of the zonal wind from current rawinsonde observations as a function of grid spacing.

As one would expect, Fig. 5 clearly shows that when the number of observations is small, a comparatively large gain is achieved by increasing the number of observations. As these observations become denser, the gain achieved from a given number of additional observations progressively decreases. Thus, at 200 mb in January, the rms interpolation error may be reduced by 4 kt, from 18 to 14 kt, by increasing the number of observations from about 150 to 500. However, a further addition of 500 stations would result in decreasing the interpolation error by less than 2 kt. A similar trend is noticeable at 200 mb in July and at 850 mb, although the curves from the latter are more flat.

The point of diminishing returns cannot be determined objectively. It depends on the purpose for which the observations are intended and on the economic or scientific benefits of a given increment of accuracy as compared to the effort and expense involved in providing the requisite additional observations to achieve this accuracy. For the purposes of forecasting by numerical models, the point of diminishing returns may be estimated by running these models with different data inputs and by determining the manner in which the accuracy of forecasts is affected by increasing or decreasing the density of observations (Alaka and Lewis 1967, 1968; Gandin *et al.*, 1967). However, the results of such experiments depend not only on the model used, but also on the season, location, and meteorological situation.

3. Gradients

Often, the accurate estimation of the gradients of a reconstructed field is equally if not more important than the correct estimation of the absolute values of the fields at specific locations.

The capability of a set of observations, subject to random errors, in determining the true gradients of meteorological fields may be assessed through the concept of efficiency (E_s) of observational systems.

Consider a regular array of discrete observations that is subject to a random error ϵ and is separated by a space or time interval τ. If σ_ϵ is the rms error of observations and σ_τ the standard deviation of the true time or space variation of the measured element in the interval τ, we may define the efficiency (E_s) of these observations (Alaka, 1970; Alaka and Elvander, 1970) as

$$E_s=1-\frac{\sigma_\epsilon}{\sigma_\tau}. \tag{12}$$

In applying the above definition, we shall restrict ourselves to cases where $\sigma_\epsilon<\sigma_\tau$. In general, σ_τ increases with τ, at least when the latter is small. Under these circumstances, for a given value of the random errors σ_ϵ, the efficiency increases as τ increases.

If τ is a space interval, σ_τ varies with the autocorrelation coefficient according to the well-known relation for the variance of a difference,

$$\sigma_\tau^2=\sigma_A^2+\sigma_B^2-2\sigma_A\sigma_B\mu_{AB}, \tag{13}$$

where σ_A^2 and σ_B^2 denote the variance of the measured element at locations A and B, respectively, and μ_{AB} is the autocorrelation coefficient between the values of this element at these locations.

If the variance is homogeneous over the region of interest, Eq. (13) becomes

$$\sigma_\tau^2=2\sigma^2(1-\mu_{AB}). \tag{14}$$

If, furthermore, the autocorrelation coefficient is assumed to be both homogeneous and isotropic, μ_{AB} becomes $\mu(\tau)$, a function only of the distance between observations. Eq. (12) then becomes

$$E_s=1-\frac{\sigma_\epsilon}{\sigma\{2[1-\mu(\tau)]\}^{\frac{1}{2}}}. \tag{15}$$

Finally, if we define an error index, then

$$\lambda=\frac{\sigma_\epsilon}{\sigma}, \tag{16}$$

$$E_s=1-\frac{\lambda}{\{2[1-\mu(\tau)]\}^{\frac{1}{2}}}. \tag{17}$$

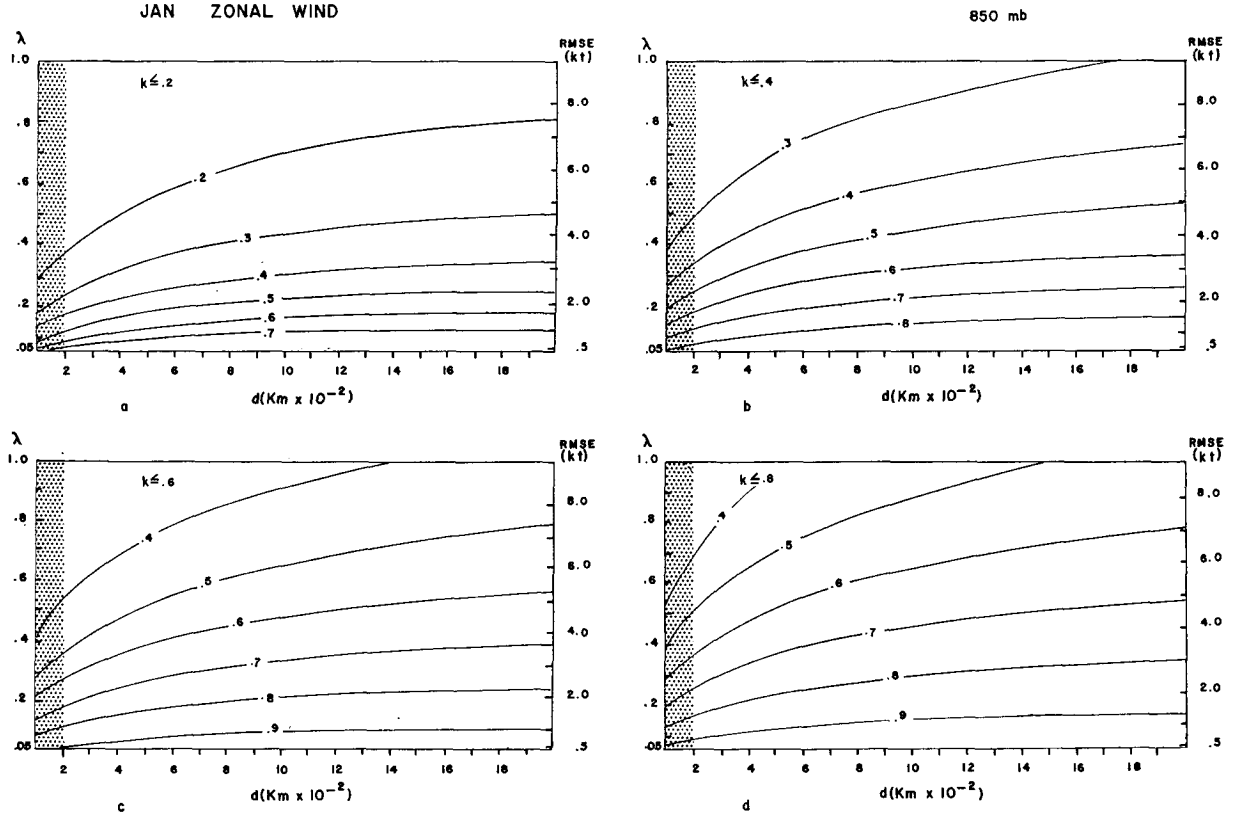

FIG. 6. The probability that the error in the measured difference between two observations of the 850-mb zonal wind, d km apart, in January, is equal to or less than a fraction k of the true difference.

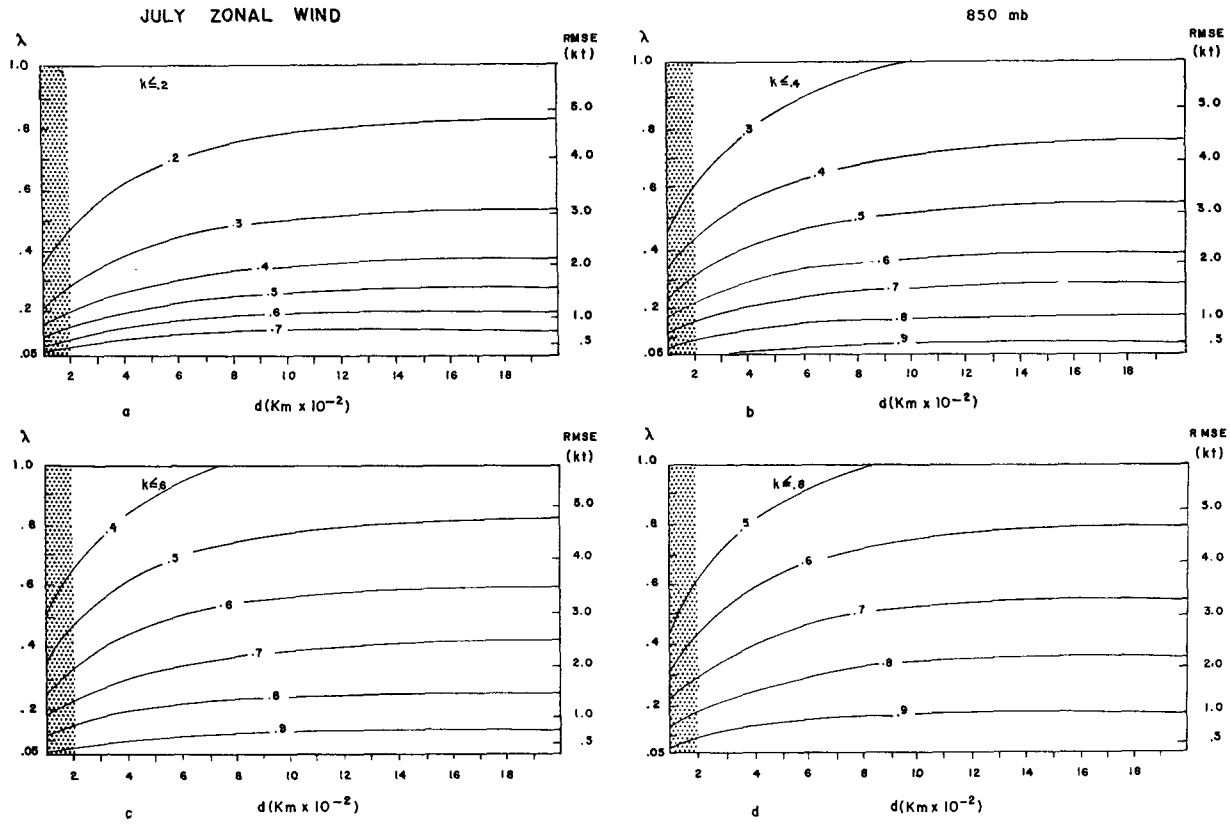

FIG. 7. Same as Fig. 5 except for July.

If τ is a time interval, $\mu(\tau)$ in the above equations denotes a time correlation coefficient with lag τ.

To appreciate the implications of the above formulation, we may express it in terms of the probability P that the error in the measured difference between two observations, separated by a time or space interval τ, does not exceed a fraction k of the true difference. The governing equation (Bessemoulin, 1960) is

$$P=1-\frac{2}{\pi}\tan^{-1}\frac{\lambda}{k}\{2[1-\mu(\tau)]\}^{-1/2}. \qquad (18)$$

The above equation assumes that the variations of the meteorological quantity under consideration are Gaussian with mean zero.

In Figs. 6 and 7, isopleths of the probability P are drawn for values of $k\leqslant 0.2$, 0.4, 0.6 and 0.8 as a function of the distance between data points and of the accuracy of the zonal wind at 850 mb in January and July. For a given value of k, the probability increases with decreasing observational errors and increasing distance between neighboring observations. Let us suppose that we have an observational system from which we can construct a lattice of interpolated values 300 km apart, with an rms error of 5 kt at 850 mb in January. According to Fig. 6a, the probability is 0.15 that $k\leqslant 0.2$, i.e., that the error in the computed difference between two consecutive grid-point values is 0.2 or less of the true difference. This probability increases to 0.32, 0.43 and 0.53 for $k\leqslant 0.4$ (Fig. 6b), 0.6 (Fig. 6c), and 0.8 (Fig. 6d), respectively. For a 500-km grid, the probabilities are 0.2, 0.4, 0.5 and 0.6, respectively, that $k\leqslant 0.2$, 0.4, 0.6 and 0.8. It will be noted that when the accuracy of the interpolated values is within 4–5 kt, the probability for any given value of k does not vary appreciably with grid distance when the latter is greater than about 500–600 km. However, as the grid resolution becomes higher, the probability becomes increasingly sensitive to the grid length, especially when the errors in the grid-point values are large.

The combined information in Figs. 5–7 allows a proper matching between the accuracy and density of the raw observations on the one hand and the grid resolution which these observations will support. It is seen that a meaningful grid resolution is largely dependent on the accuracy of the interpolated values. This accuracy, in turn, is dependent more on the density of the raw observations than on their accuracy. It follows, if the results described here are at all typical of other meteorological elements in different localities and seasons, that there is not a one-to-one correspondence between the appropriate resolution of the raw observations and that of the reconstructed grid. The representative distance between the raw observations must be

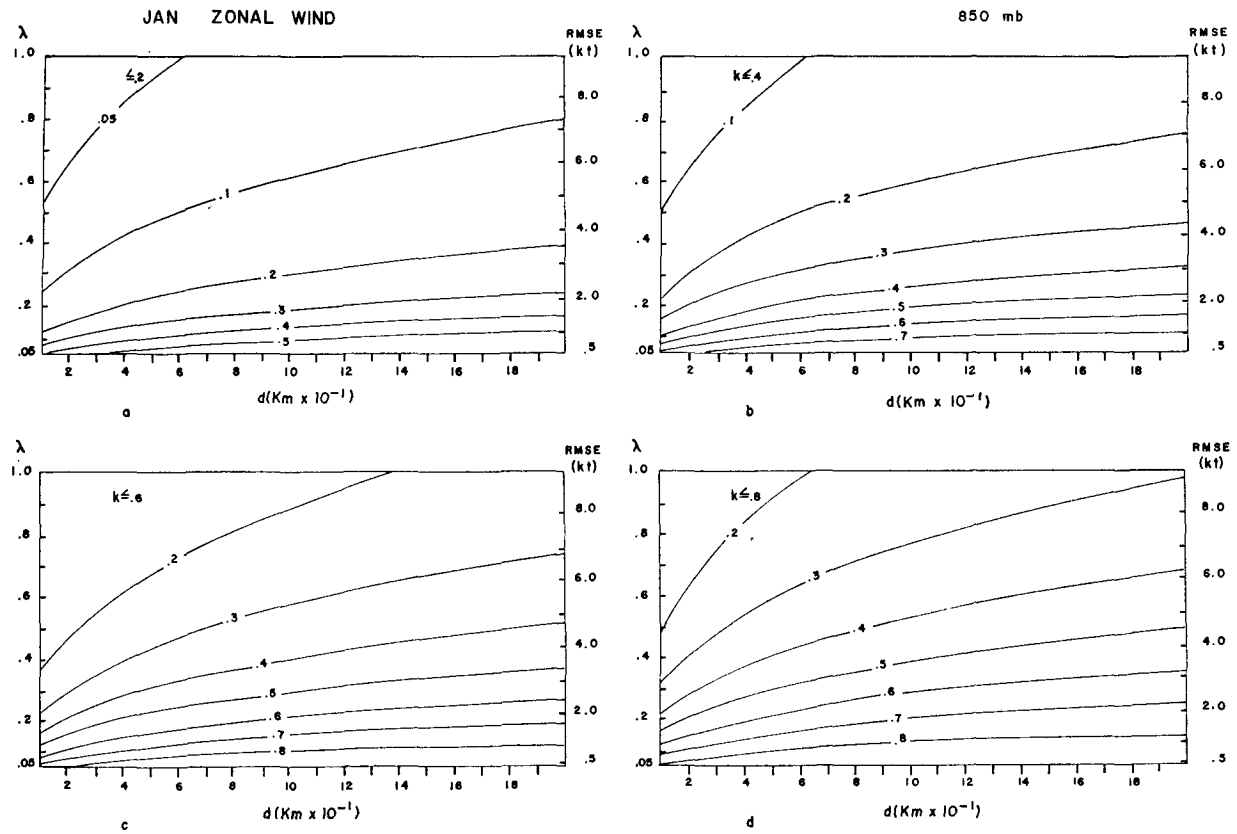

FIG. 8. Enlargement of the shaded part of Fig. 6.

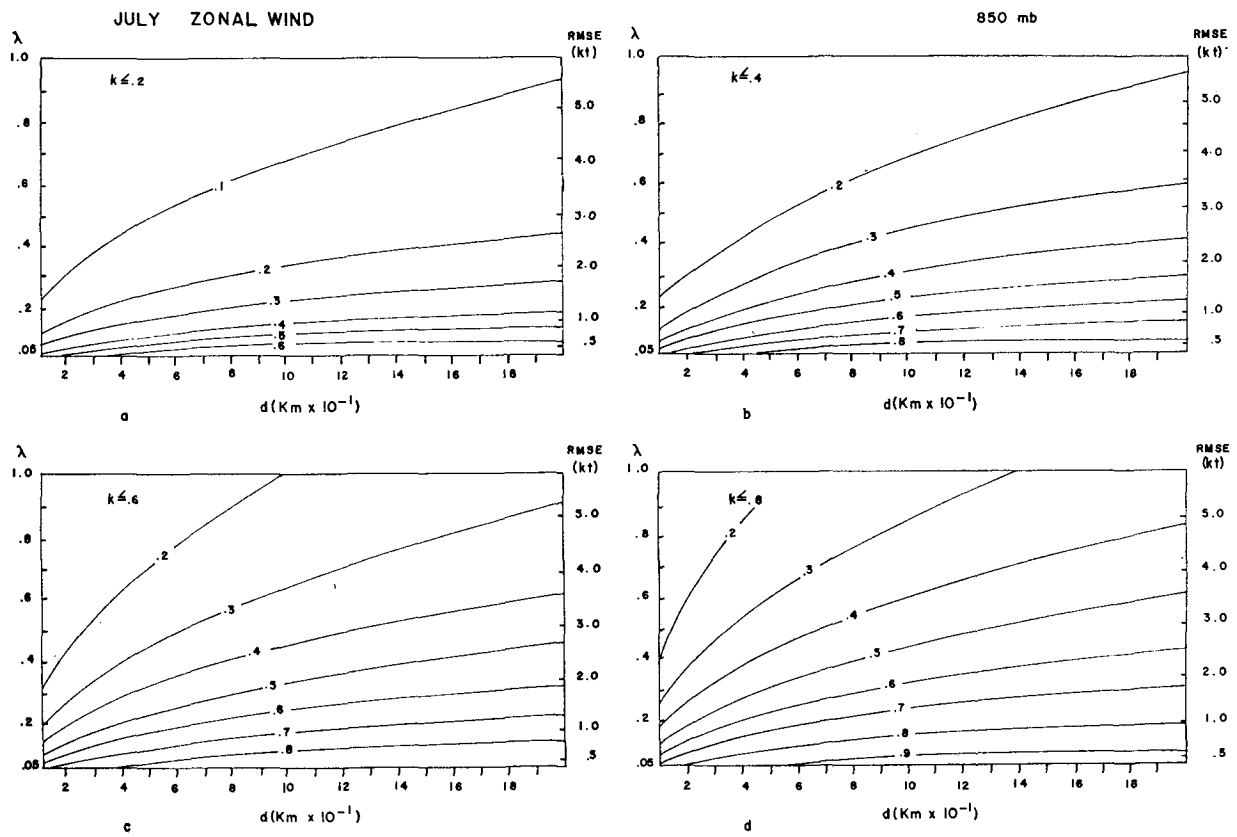

FIG. 9. Enlargement of the shaded part of Fig. 7.

smaller than that between the reconstructed grid points if the field gradients are to be determined with reasonable accuracy.[3]

The above analysis may be extended to determine the accuracy with which second and higher order differences may be computed from raw observations of any given accuracy and density.

4. High-resolution sampling

The concepts developed above may also be used to guide planners of high-resolution meteorological field experiments on the proper matching of density and accuracy of observations. Strictly speaking, the application of the concepts to high-resolution atmospheric sampling requires statistics of a correspondingly high degree of resolution. The autocorrelations used in the previous sections were computed from observations which were too far apart to resolve features on a scale of less than about 200 km. They do not therefore take into consideration such vigorous small-scale circulations which are known to exist within hurricanes and other organized convective systems. The results of this section are thus limited to conditions when no vigorous convective activity exists.

Figs. 8 and 9 are enlargements of the shaded parts of Figs. 6 and 7. The scale of the abscissa is now in tens instead of hundreds of kilometers. Fig. 8a shows that at 850 mb in January, if we can measure the zonal component of the wind with an accuracy of 3 kt and if we have two observations 100 km apart, then there is only 0.22 probability that $k \leqslant 0.2$. When $k \leqslant 0.4$, 0.6 and 0.8, the probability increases to 0.34, 0.49 and 0.57, respectively. To achieve a probability of 0.4 that the error in the measured difference is equal to or less than 0.2 of the true difference, the accuracy of the measurement must be within 1 kt. The situation in July, shown in Fig. 9, is very similar.

Fig. 10 relates to the temperature field at 850 mb in July. Fig. 10a shows that if the distance between two observations is 100 km and the rms observation error is 1C, there is a 0.15 probability that $k \leqslant 0.2$. On the other hand, if the rms observation error is 0.1C, the probability for $k \leqslant 0.2$ is greater than 0.6. The probability is more than 0.9 that $k \leqslant 0.6$ (Fig. 10c).

5. Effect of optimum smoothing

Alaka and Elvander (1970, 1972) have shown that it is possible to reduce the rms errors of a set of observa-

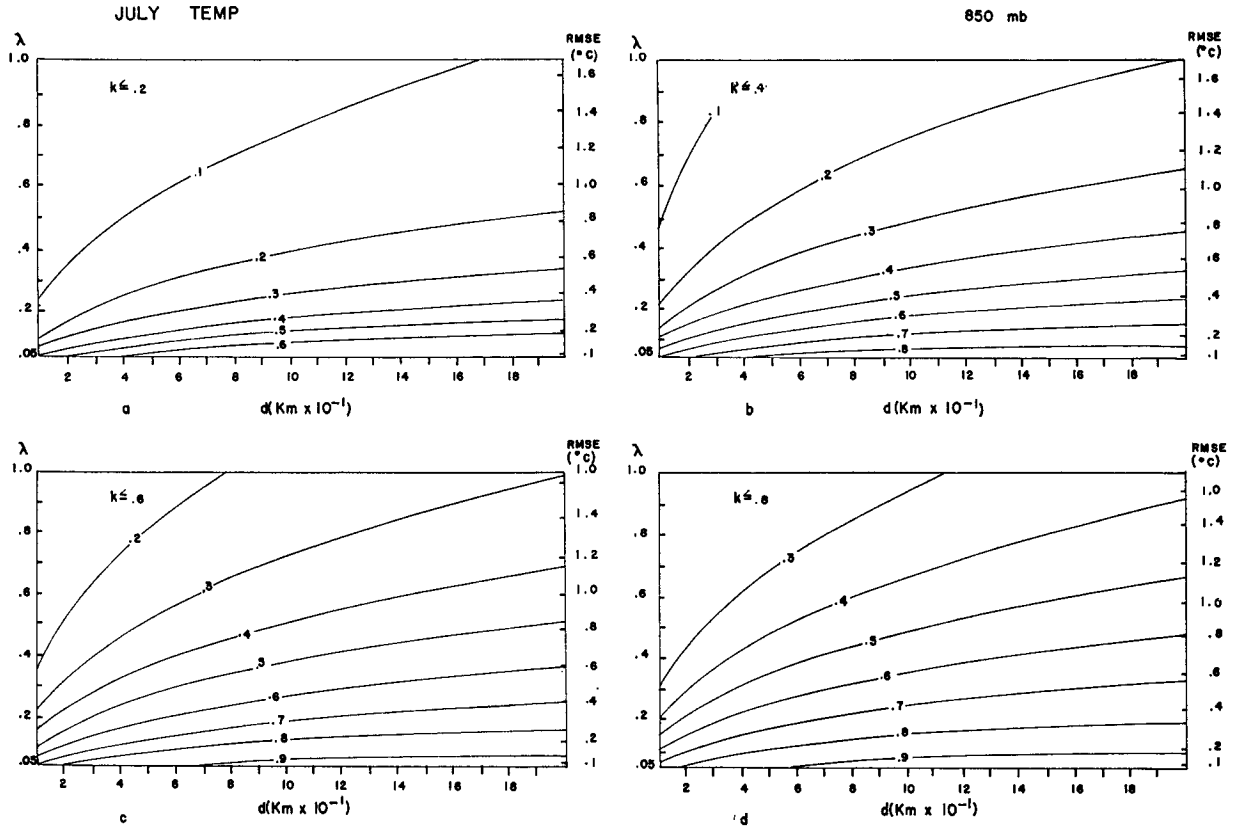

FIG. 10. Isopleths of probability that the error in the measured difference between two temperature observations at 850 mb in July is equal to or less than a fraction k of the true difference, as a function of the rms random errors of the observations and of the distance (in tens of kilometers) between them.

[3] This conclusion relates to the information content of the interpolated values and is distinct from the computational problem of truncation which is alleviated by fine-mesh grids.

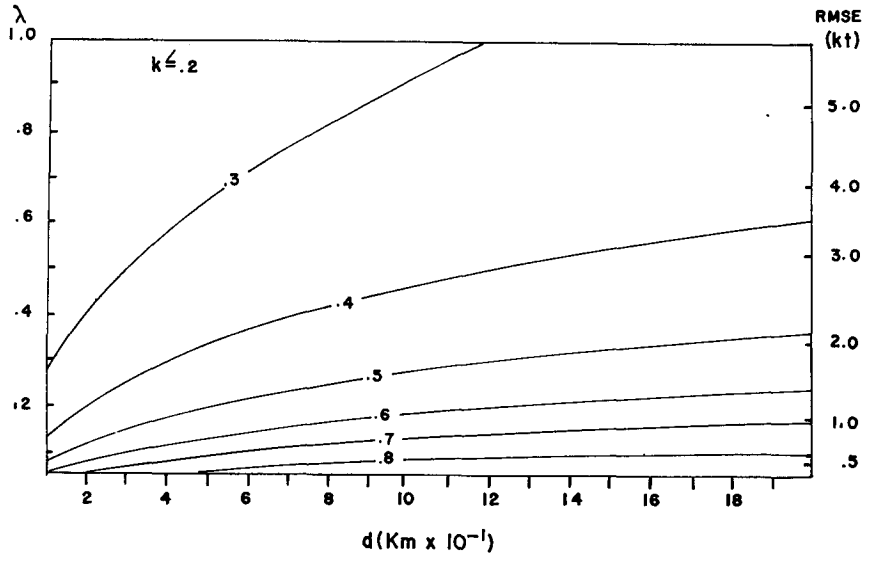

FIG. 11. Same as Fig. 9b except that the observations are optimally smoothed.

tions by optimum smoothing. This involves a weighted linear combination of each observation with neighboring observations, the proper weights being determined by application of Eq. (10).

Fig. 11 is identical with Fig. 9b except that the latter relates to observations which have been smoothed by optimum combination with the eight closest observations. It is seen that, other things being equal, the probability is generally higher that $k \leqslant 0.4$. The increase in probability is more noticeable when the rms error of the raw observations is relatively high; it diminishes with increasing observational accuracy and all but vanishes when the rms error of the original observation is less than 1 kt.

6. Conclusions

We have attempted to develop and to illustrate a methodology which we hope will be of use in planning meteorological data acquisition experiments including experiments which involve high-resolution atmospheric sampling. The significance of investigations of this type lies in the insight they provide planners into the options at their disposal. Thus, if the intent of the field experiments is to delineate the broad-scale atmospheric features, the procedures we have described should help identify the point of diminishing returns for instrumental accuracy. Conversely, if only a given instrumental accuracy is obtainable, these same procedures should provide an estimate of the maximum useful sampling resolution.

The present study is by no means exhaustive. It must be supplemented by similar computations for other meteorological elements, seasons, locations and levels. In addition, with the help of the appropriate lag correlations, the proper relation between observational accuracy and frequency could be determined.

However, we hope that the present results clearly point to the care which planners must exercise to avoid, on the one hand, the expense of superfluous observational accuracy for large-scale atmospheric sampling and, on the other hand, to ensure that the observations are sufficiently accurate for meaningful high-resolution sampling. It is obvious that one and the same set of observational standards cannot be appropriate for atmospheric sampling on all scales.

Acknowledgments. The authors are indebted to Brenda Eastridge and Denis Sakelaris of the Techniques Development Laboratory for their capable assistance in the preparation of the manuscript.

REFERENCES

Alaka, M. A., 1970: Theoretical and practical considerations for network design. *Meteor. Monogr.*, **11**, No. 33, 20–27.

——, and F. Lewis, 1967: Numerical experiments leading to the design of optimum global meteorological networks. Tech. Memo. WBTM TDL-7, ESSA, Weather Bureau, Washington D. C., 14 pp.

——, and ——, 1968: Numerical experiments pertinent to the design of optimum aerological networks. *Proc. Symp. Numerical Weather Prediction*, Tokyo, Japan Meteor. Agency, V9-V18.

——, and R. C. Elvander, 1970: Current high-altitude observations—investigation and possible improvement. Tech. Memo. WBTM TDL-36, ESSA, Weather Bureau, Silver Spring, Md., 24 pp.

——, and ——, 1972: Optimum interpolation from data of mixed quality. *Mon. Wea. Rev.*, **100** (in press).

Bessemoulin, J., 1960: Rapport préliminaire du groupe de travail de la Commission de Météorologie Synoptique sur les réseaux. Note Tech. No. 30, WMO, Geneva, 91 pp.

COSPAR Working Group 6, 1971: The feasibility of the First Garp Experiment (FGGE) and the criticality of initiating

systems planning. Report to the Joint Organizing Committee, GARP, 42 pp., Annexes A–M.

Elvander, R. C., and M. A. Alaka, 1970: Some considerations of meteorological networks design in the tropics. *Preprints of Papers, Symp. on Tropical Meteorology*, Honolulu, Hawaii, Amer. Meteor. Soc., BX 1–BX 8.

Gandin, L. S., 1963: *Objective Analysis of Meteorological Fields*. Leningrad, USSR, Hydrometeor. Publ. House (English version, Israel program for Scientific Translations, 1965), 242 pp.

——, S. A. Mashkovitch, M. A. Alaka and F. Lewis, 1967: Design of optimum networks for aerological observing stations. WWW Planning Rept., No. 21, WMO, Geneva, 58 pp.

Steinitz, G. *et al.*, 1970: Optimum station networks in the tropics. Rept., ESSA Contract E-267-(68)N, Israel Meteor. Service, Bet Dagan, 71 pp.